Nuclear-Structure and Hyperfine-Field Studies with Mo^{95} †

Peter Bond* and S. Jha‡
Case Western Reserve University, Cleveland, Ohio 44106
(Received 30 March 1970)

Excitation functions for (α, xn), $(\alpha, \alpha n)$, and $(\alpha, 2p)$ reactions upon niobium targets have been measured for incident α-particle energies from 15 to 41 MeV. Excited states in Mo^{95} have been studied by observing the decay of the 61-day isotope Tc^{95m}, which was produced by the $Nb^{93}(\alpha, 2n)$ reaction. The energies and the intensities of the γ rays resulting from this decay have been measured. The angular-correlation coefficients of the two strongest cascades in Mo^{95} have been found to be $A_{22} = -0.292 \pm 0.005$ and $A_{44} = -0.001 \pm 0.006$ for the 582–204-keV cascade, and $A_{22} = -0.196 \pm 0.006$ and $A_{44} = -0.003 \pm 0.008$ for the 835–204-keV cascade. The mean life of the 204-keV state has been measured by the delayed-coincidence technique and found to be 1.09 ± 0.02 nsec. The g factor of the 204-keV state has been measured to be -0.26 ± 0.02. A summary of a number of calculations concerning the nuclear structure of Mo^{95} is given, and some predictions of the Kisslinger-Kumar model of near-spherical nuclei for Mo^{95} are presented. The technique of perturbed angular correlations has been used to measure the hyperfine fields at the molybdenum nucleus in iron and nickel hosts. These fields have been found to be B_{eff}(Mo in Fe) $= -236 \pm 19$ kG and B_{eff}(Mo in Ni) $= -29.9 \pm 5.1$ kG at 55°C.

INTRODUCTION

The excited states of Mo^{95} are well suited to experimental studies by β-decay and nuclear-reaction techniques. Because of the occurrence of nuclear isomerism, the decay of Tc^{95} from its ground state ($\frac{9}{2}+$) and from the isomeric state ($\frac{1}{2}-$) feeds both the high- and low-spin states of Mo^{95}. In addition, nuclear-reaction data on the excited states of Mo^{95} can be obtained because neighboring isotopes are stable. However, despite rather numerous studies[1-5] of the electron-capture decay of Tc^{95} and of pickup and stripping reactions,[6-9] several discrepancies in the data have persisted.

We have chosen to produce Tc^{95m} by α bombardment upon monoisotopic niobium. We have measured the energies and intensities of the γ rays from the decay of Tc^{95m} and have found general agreement with the recent results of Chilosi, Eichler, and Aras (CEA).[5] Unperturbed angular correlations for the two strongest cascades in the decay of Tc^{95m} were measured in an effort to resolve the large discrepancy in previous results.[10,11] The mean life of the 204-keV state was measured electronically and found to be in agreement with the most recent results.[12,13] The technique of perturbed angular correlations was used to measure the g factor of the 204-keV state. Our value for the g factor was found to differ considerably from that of the previous measurement.[14]

The nuclear structure of Mo^{95} is not well understood. Three previous calculations[15-18] dealing with its structure are summarized. We have applied the Kisslinger-Kumar model[19] of near-spherical nuclei, which might be expected to be suitable in this region of the Periodic Table, but have found that this model also fails to account for rather important features of Mo^{95}.

We have used Mo^{95} also to study a rather different phenomenon, that of the large hyperfine fields created at nonmagnetic solute nuclei in ferromagnetic hosts. We have measured the hyperfine field at the molybdenum nucleus in an iron host by the perturbed-angular-correlation technique and have found agreement with the previous spin-echo results.[20] We have measured this field also in a nickel host and have found it to be in reasonable agreement with the empirical predictions of Shirley, Rosenblum, and Matthias.[20]

Source Preparation

In order to obtain the cleanest possible source of Tc^{95m}, the excitation functions for $Nb^{93}(\alpha, 2n)$-Tc^{95} as well as for (α, n), $(\alpha, 3n)$, $(\alpha, \alpha n)$, and $(\alpha, 2p)$ reactions were measured at the National Aeronautical and Space Administration-Lewis Research Center. For the excitation-function measurement, 13 niobium metal foils, each 21.8 mg/cm², were stacked and subjected to 3 μA h of 41-MeV α particles. The activity in each foil was then investigated with Ge(Li) detectors[21] which, in contrast to the previous excitation-function study,[22] permitted the use of a single γ ray to identify each product nucleus despite the wealth of γ rays between 700 and 1000 keV.

The cross section for the reaction $Nb^{93}(\alpha, n)$-$Tc^{96g,96m}$ was evaluated by observing the 813-keV γ ray, which occurs with an intensity of 85% in the

decay of Tc^{96g} and with an intensity of 83% in the decay of Tc^{96m}.[23] The reason for not treating Tc^{96g} and Tc^{96m} separately was that 98% of the Tc^{96m} decay is to Tc^{96g}. The activity of Tc^{95g} from the reaction $Nb^{93}(\alpha, 2n)$ was found from the intensity of the 766-keV γ ray[8] and that of Tc^{95m} from the intensity of the 204-keV γ ray. The yield of Nb^{93}-$(\alpha, 3n)Tc^{94g}$ was found from the intensity of the 703-keV γ ray.[24] The amount of Tc^{94m} produced in the $(\alpha, 3n)$ reaction was identified from the intensity of the 871-keV γ ray. Since both the 871- and 849-keV γ rays occur with 100% intensity in the decay of Tc^{94g}, the difference in the intensity of the 849- and 871-keV γ rays was used to determine the activity of Tc^{94m}. The 935-keV γ ray in the decay[25] of Nb^{92} was used to measure the yield in the $Nb^{93}(\alpha, \alpha n)$ reaction. The yield of Nb^{95} in the reaction $Nb^{93}(\alpha, 2p)$ was found by measuring the 766-keV γ ray[25] about 30 days after the bombardment, when the only other contribution to this γ-ray intensity was from the decay of Tc^{95m} and could be accounted for. Small amounts of activities resulting from the reactions $Nb^{93}(\alpha, 4n)Tc^{93}$ and $Nb^{93}(\alpha, \alpha 2n)Nb^{91}$ were observed but were too feeble for meaningful excitation-function studies.

Once the decay rates were found, they were corrected for the absolute efficiencies of the Ge(Li) detectors, which were determined by the use of a calibrated Mn^{54} (835-keV) source and the relative-efficiency curves for the detectors given in Fig. 1. The cross sections were then determined from the corrected decay rates. The results for the excitation functions are plotted in Fig. 2 against the mean energy of the α beam. These average energies were calculated by the use of the Bragg-Kleeman rule and the known range-energy relation of α particles through molybdenum.[26] Cross sections for the production of Nb^{95} were very small and are given in Table I. The errors in the absolute cross sections are about 20% except in the case of $(\alpha, 2p)$ cross sections, where the errors are larger. The errors in the relative cross sections are about 10%.

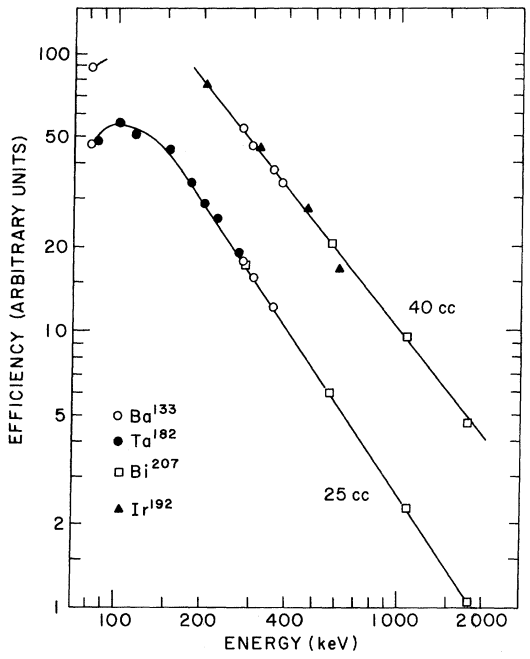

FIG. 1. Relative efficiency of detection as a function of the γ-ray energy for the 25- and 40-cc detectors.

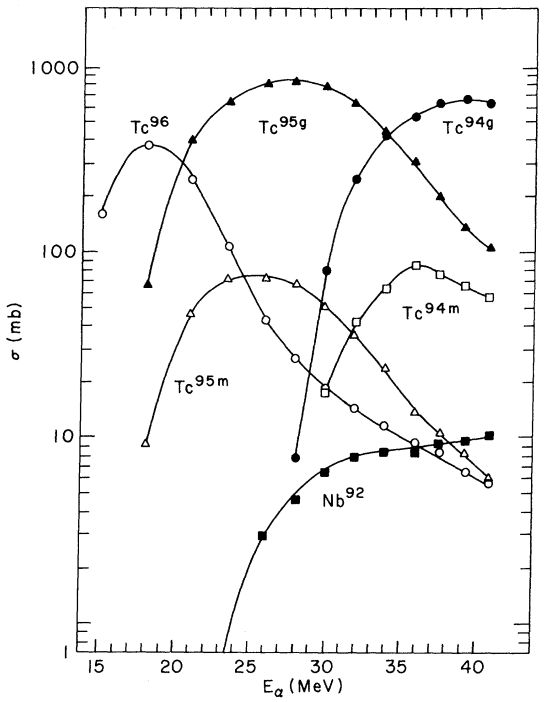

FIG. 2. The excitation function for the reactions produced by α particles on niobium.

The primary interest in the study of the excitation function was to produce a pure source of Tc^{95m} for further studies, and no attempt was made to analyze the structure of the excitation functions. However, the general agreement of the (α, xn) cross sections in this work and that of Matsuo *et al.*[22] is good. The production of the niobium isotopes in the α-particle bombardment was not reported in that work.

Sources of Tc^{95m} in a metallic environment were chosen from those Nb foils which, after aging for about 60 days, had negligible activity of niobium isotopes. The other niobium foils were dissolved in a mixture of concentrated nitric and hydroflu-

TABLE I. Cross section $Nb^{93}(\alpha, 2p)Nb^{95}$.

Energy (MeV)	41.0	39.3	37.6	35.9	34.0
σ(mb)	0.35	0.35	0.30	0.29	<0.1

oric acids. Concentrated ammonium hydroxide and hydrogen peroxide were added until the solution became slightly basic in order to precipitate niobium, presumably in the form of Nb_2O_5. After centrifuging, the ratio of the activity of Tc^{95m} in the supernatant to that in the precipitate was about 4:1. There was no noticeable niobium activity.

Decay of Tc^{95m}

We feel that no previous study of the decay of Tc^{95} has been made with as pure a source as described above. One of the spectra of the decay γ rays of Tc^{95m}, taken with a 40-cc Ge(Li) detector, is shown in Fig. 3. Energies and relative intensities for the γ rays are shown in Table II, along with the results of the previous two Ge(Li) studies. The energies of corresponding γ rays are in excellent agreement with CEA[5] and lower in energy than previous workers by about 2 keV.

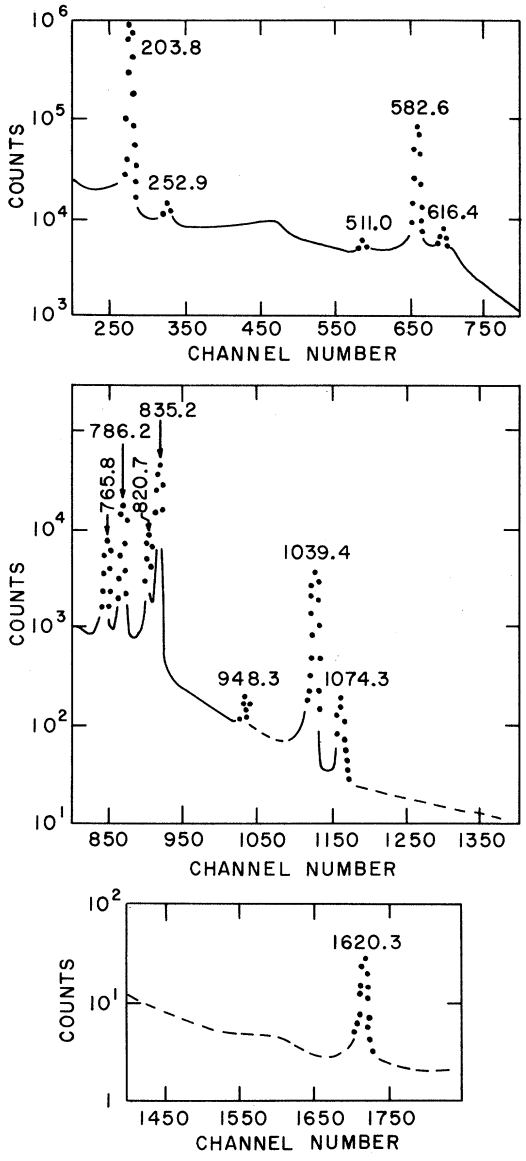

FIG. 3. The spectrum of the γ rays from Tc^{95m} taken with 40-cc Ge(Li) detector.

There has been some question about the 765.8- and 786.2-keV γ rays. Unik and Rasmussen[2] reported seeing conversion-electron lines corresponding to 763- and 768- and 784- and 788-keV γ rays. Other conversion-electron studies[3,4] have not resolved these two sets of lines. If the conversion coefficients for the γ rays were comparable and the intensities were as reported by Unik and Rasmussen, it is almost certain that at least a broadening of the 765.8- and 786.2-keV peaks would be seen in Ge(Li) detectors. This broadening has not been observed in this work nor in that of CEA.[5] We were unable to conclude whether the three weak γ rays at 219, 1057, and 1222 keV reported by CEA are in the decay.

Coincidence measurements were made with a NaI-Ge(Li) system and confirmed the well-known cascades. In coincidence with the 204-keV γ ray are the 582-, 616-, and 835-keV γ rays. The 786- and 582-keV γ rays are in coincidence with the 253-keV γ ray.

Cretzu, Hohmuth, and Schintlemeister (CHS)[4] have shown that there are two positron branches in the decay of Tc^{95m} and estimated the total positron branching to be $(0.42 \pm 0.05)\%$. The theoretical values for the ratio of K capture to positrons can be used to find the percentage of electron captures feeding the ground and first excited state. CHS find 14.3% of the electron captures feed the ground state and 7.2% feed the 204-keV level directly.

We have checked the total positron branching by

TABLE II. γ rays in the decay of Tc^{95m}.

Energy (keV)	Relative γ-ray intensity This work	Ref. 5	Ref. 1
203.8	100	100	100
219.4	...	0.12	...
252.9	0.8	1.1	0.8
582.6	50	55	50
616.4	2.4	2.4	1.8
765.8 [a]	6	6	7.7
786.2	15	15	15
820.7	8.8	8	11
835.2	43	45	39
948.3 [a]	0.10	...	0.12
1039.4	5.2	5	4.3
1057.0	...	0.022	...
1074.4 [a]	0.23	...	0.20
1222.5	...	0.013	...
1620.3	0.061	0.065	...

[a] Due to Tc^{95g} in equilibrium.

comparing the annihilation coincidence rate with the 835–204 and 582–204 coincidence rates. The average of these measurements indicates a total positron branching of $\beta^+ = (0.47 \pm 0.06)\%$, which is in good agreement with the value found by CHS.[4]

Figure 4 shows a decay scheme derived from the percentage of electron captures to the lowest two states found by CHS and the relative intensities of γ rays found in our work. The percent of each transition is shown in the diagram. Only the 204-keV transition is appreciably converted and the conversion coefficient of 0.054 was used in constructing the decay scheme. The percentage of the isomeric transition to Tc^{95g} was deduced from the intensity of the 766-keV γ ray and the assumption that 94% of the decay of Tc^{95g} proceeds through the 766-keV level.[5]

Levels of Mo^{95} are assumed to be due mainly to the odd neutrons, and since the single-particle levels which are being filled have positive parity, it is assumed that there are no low-lying negative-parity states. The assignments of $\frac{5}{2}+$ to the ground state, $\frac{3}{2}+$ to the 204-keV level, and $\frac{7}{2}+$ to the 765.8-keV level come from previous workers.[27-29] Spin assignments to the 786.2- and 1039.4-keV level are discussed below under angular correlations.

Most studies[6-8] of $Mo^{94}(d,p)Mo^{95}$ have suffered from a lack of good energy resolution so that both energy and spin assignments to the levels were uncertain. However, a recent very high-resolution study of this reaction[9] has confirmed both the energy and spin assignments of the levels seen in the decay, as well as adding many higher-energy levels.

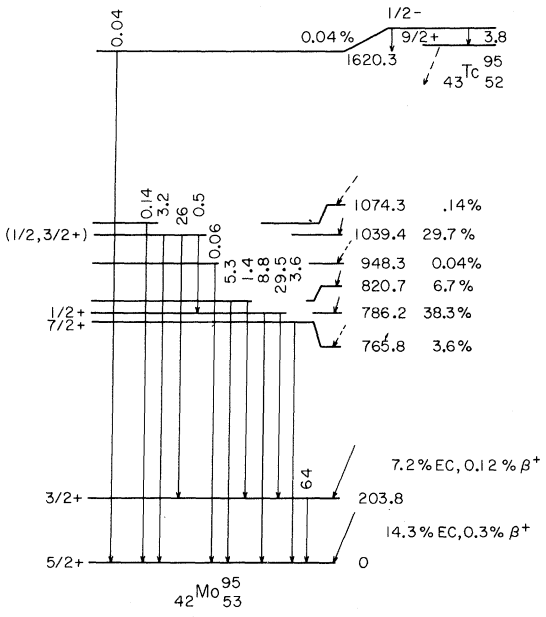

FIG. 4. The decay scheme of 60-day Tc^{95m}

TABLE III. Results for Mo^{95} 204-keV mean life.

Mean life (nsec)	Ref.	Method
1.11 ± 0.04	a	Delayed coincidence (centroid)
1.10 ± 0.09	28	Coulomb excitation
1.03 ± 0.10	b	Pulsed beam
1.17 ± 0.06	12	Delayed coincidence (slope)
1.09 ± 0.02	13	Delayed coincidence (slope)
1.07 ± 0.02	14	Delayed coincidence (slope)
1.09 ± 0.02	This work	Delayed coincidence (slope)

[a] M. J. Quidort, Compt. Rend 246, 2119 (1958).
[b] R. E. Holland and F. J. Lynch, Phys. Rev. 121, 1464 (1961).

Our study and the other two most recent studies of Mo^{95} all indicate[5,9] that there are fewer levels in Mo^{95} around 800 keV than previously reported.[25]

Lifetime of 204-keV Level

Because the previous values for the mean life of the 204-keV level have covered a rather large range (see Table III) and because of the importance of this mean life to the measurement of the gyromagnetic ratio of the 204-keV level, we felt that an accurate measurement of this lifetime was warranted.

Both of the strong γ-ray cascades 582-204 and

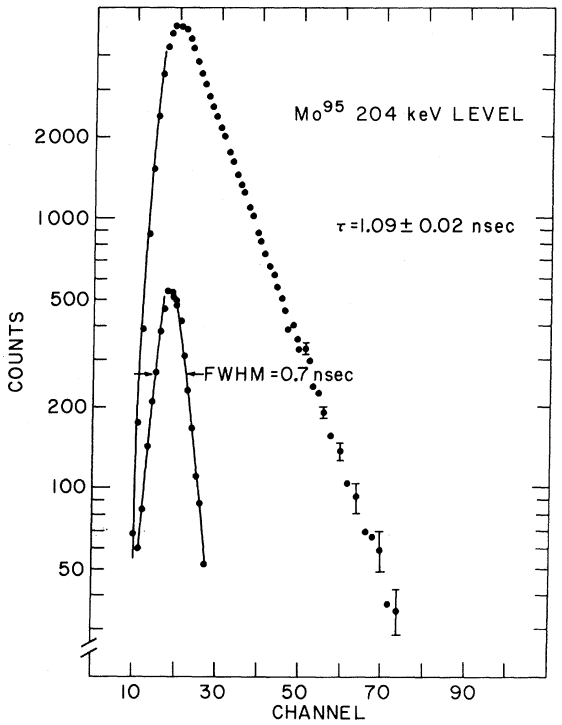

FIG. 5. The 582–204-keV delayed-coincidence curve for the measurement of the mean life of the 204-keV state.

835-204 were used to measure the mean life by the delayed-coincidence technique. For most of the data discussed below, γ rays were detected by $1\frac{1}{2}$-in.$\times$1-in. Naton 136 plastic scintillators optically coupled to RCA 7746 photomultiplier tubes. Pulses from the photomultiplier anode triggered a tunnel-diode discriminator and Schmitt trigger of our own design before feeding a time-to-amplitude converter (TAC) of the Bell type.[30] Additional data were accumulated with 1-in.$\times$1-in. Naton 136 scintillators coupled to XP 1021 photomultipliers feeding an ORTEC TAC.

One of the delayed-coincidence curves for the Mo^{95} 204-keV level and a prompt-resolution curve, taken using a Co^{60} source with the same energy selection, are shown in Fig. 5. Calibration of the TAC was accomplished in two ways. Pulses from a pulse generator were fed to the tunnel-diode discriminators through an air-dielectric delay line in order to vary the time between the TAC start and stop pulses. Several previously measured mean lives were remeasured as an additional check of the calibration, e.g., for the 155-keV level in Os^{188} we obtained $\tau_m = 1.03 \pm 0.03$ nsec. The calibrations indicated linearity to within about 2%.

Our result for the mean life of the 204-keV level is $\tau_m = 1.09 \pm 0.02$ nsec, which agrees very well with the most recent measurements.[12,13]

Angular Correlations

Previous angular correlations performed on the 582-204 and 835-204 cascades were not in good agreement with each other (see Table IV). The angular-correlation coefficients must be known accurately for a confident spin assignment to the levels in question and for our g-factor measurement; hence, we have measured these cascades again.

Two 7.6-cm$\times$7.6-cm NaI(Tl) crystals[31] were used to measure most of the angular correlations. Both the singles and coincidence spectra of the movable counter were stored in a Victoreen 400-channel analyzer used in conjunction with a routing system designed by Shera and Casper.[32] The gain of the gate counter was stabilized with a feedback system,[33] and the single channel of this counter was monitored with a scaler as an additional check against window drift. The use of the multichannel analyzer provided several advantages over the single-channel method used by other workers. There is little problem of gain shift in the movable counter; both the 582-204 and 835-204 angular correlations could be performed simultaneously, and several problems, which exist in the 582-204 cascade and could account for the discrepancies in the previous results, could be better accounted for here. The annihilation peak could be resolved on the analyzer so that the correlation at 180° did not have to be avoided. The contribution to the 582-keV photopeak from the Compton distribution of the 835-keV γ ray was accurately measured in this experiment by using a source of Mn^{54} which has a single 835-keV γ ray, almost exactly the energy involved in the correlation. This single-line source was also used to estimate the scattering of the four γ rays having an energy about 800 keV. These γ rays can backscatter into the 204-keV gate leaving a false coincidence count under the 582 photopeak. This leads to an asymmetric false correlation. In order to reduce these scattered γ rays, lead shielding was placed around the gate counter and 70-mil lead was placed on the face of the higher-energy detector to reduce the backscatter γ rays without greatly reducing incident γ rays having energies over 500 keV. In order to reduce the geometrical corrections and the scattering, the correlations were performed at distances of 14 and 20 cm.

A NaI-Ge(Li) system was also used to perform the two angular correlations. The source was placed at about 10 cm from a 25-cc Ge(Li) detector so that geometrical corrections for that detector were small. Both the scattered γ rays and the Compton distribution from the 835-keV γ ray could be directly observed and corrected for because of the superior energy resolution of the Ge(Li) detector.

The angular correlations were measured for

TABLE IV. Angular-correlation results for Mo^{95}.

System	Source	582 −204 keV A_{22}	582 −204 keV A_{44}	835 −204 keV A_{22}	835 −204 keV A_{44}	Ref.
NaI-NaI	Liquid	-0.216 ± 0.010	~0	-0.162 ± 0.012	~0	10
NaI-NaI	Metal	-0.321 ± 0.017	~0	-0.195 ± 0.006	~0	11
NaI-NaI	Liquid	-0.250 ± 0.010	$+0.007 \pm 0.015$			12
NaI-Ge(Li)	Metal	-0.307 ± 0.018	~0	-0.190 ± 0.020	~0	This work
NaI-NaI	Liquid	-0.284 ± 0.009	$+0.009 \pm 0.011$	-0.185 ± 0.010	-0.004 ± 0.012	This work
NaI-NaI	Metal	-0.292 ± 0.005	-0.001 ± 0.006	-0.196 ± 0.006	-0.003 ± 0.008	This work

Tc^{95m} sources in both niobium foil and liquid surroundings. The correlations, measured with the NaI detectors, are shown in Fig. 6, and the results for the angular-correlation coefficients, corrected for geometrical effects,[34] are shown in Table IV. Although the theoretical value of A_{44} is zero (owing to the spin-$\frac{3}{2}$ intermediate state), the results were fitted to the full form of the angular distribution $W(\theta)=1+A_{22}P_2(\cos\theta)+A_{44}P_4(\cos\theta)$ to show that, experimentally, A_{44} is zero. The fact that A_{44} turned out to be so small means that the value of A_{22} would not be significantly changed if the correlation were fitted to only $1+A_{22}P_2(\cos\theta)$. The values of A_{22} for both correlations in the liquid source are somewhat smaller than in the foil source, but the uncertainties in the measurements do not permit a conclusion as to whether there is any real attenuation in the liquid.

Because the spin-$\frac{1}{2}$ isomeric state of Tc^{95} feeds the 786- and 1039-keV levels so strongly, one can conclude that these levels have a spin of either $\frac{1}{2}$ or $\frac{3}{2}$. Stelson and McGowan[28] have shown the mixing ratio of the 204-keV γ ray is negative. If we also take their value of $B(E2, \frac{3}{2}\rightarrow\frac{5}{2})=(0.054\pm0.005)\times e^2\times10^{-48}$ cm^4 and use the lifetime measured in this work, we find that the mixing ratio of the 204-keV γ ray is $\delta=-0.60\pm0.05$. Figure 7 shows the theoretical values of A_{22} for the spin sequences $\frac{1}{2}$-$\frac{3}{2}$-$\frac{5}{2}$ and $\frac{3}{2}$-$\frac{3}{2}$-$\frac{5}{2}$ plotted against $\delta_1'\equiv\delta_1(1+|\delta_1|)$ (we have chosen $\delta_2=-0.60$). The experimental values of A_{22} for the two cascades are shown by the cross-hatched areas. Conclusions from these data concerning the spin assignments and multipolarities of the γ rays are shown in Table V.

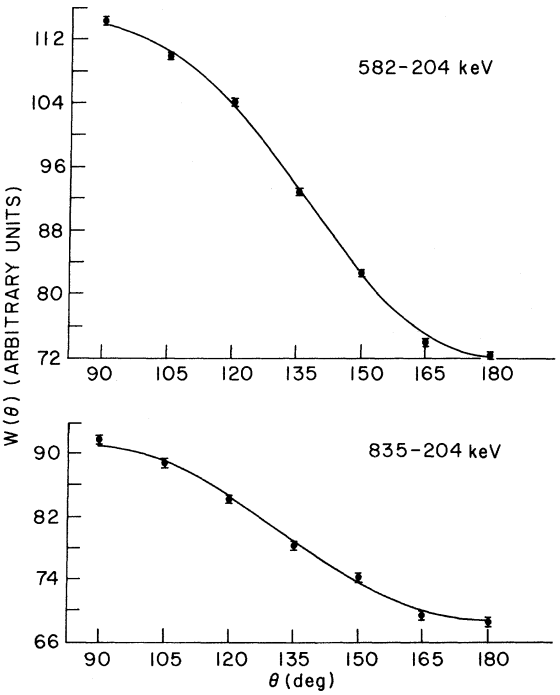

FIG. 6. Unperturbed angular correlations for the 582–204-keV and 835–204-keV cascades. The solid lines represent the least-squares fit to the data.

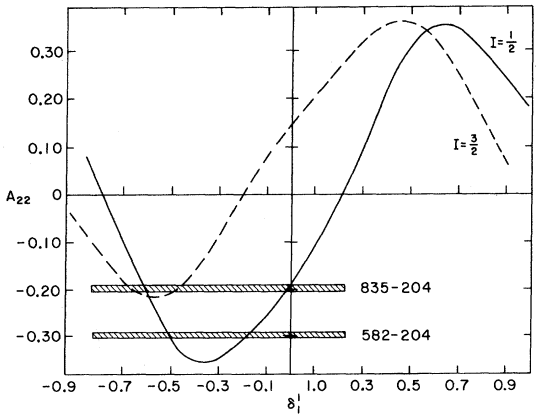

FIG. 7. The theoretical and experimental values of A_{22} plotted against δ_1' where $\delta_1'=\delta_1(1+|\delta_1|)$. The dashed theoretical curve is for spin of the 786-keV state equal to $\frac{3}{2}$, and the solid curve represents the values of A_{22} appropriate to spin $\frac{1}{2}$ for the 786-keV state. The cross-hatched areas represent the experimental values.

In an effort to obtain more information from the angular correlations, we combine the relative intensities found in this work with the conversion-electron intensities of two workers.[3,4] These conversion coefficients indicate that the 582-keV γ ray is almost pure $M1$. Unfortunately, the results for the 835-keV level are not helpful, because at that energy the conversion coefficients for $M1$ and $E2$ are almost equal. We can conclude, however, that the 786-keV level has spin $\frac{1}{2}$ and the mixing ratio of the 582-keV γ ray is -0.23 ± 0.06. The 1039-keV level can be either $\frac{1}{2}^+$ or $\frac{3}{2}^+$ with a large or small mixing ratio. Reaction data indicate that this level has spin $\frac{1}{2}^+$.[9]

The 253-786-keV cascade is very weak, and no attempt was made to see if it did indeed have the isotropic distribution that one would expect for a cascade passing through a spin-$\frac{1}{2}$ intermediate level.

g Factor of 204-keV Level

Because of the rather short mean life of the 204-

TABLE V. Conclusions from angular-correlation data.

Level (keV)	Spin	γ ray (keV)	δ	$E2/M1$
786	1/2	582	−0.23 or −1.1	0.04 or 1.2
	3/2	582	Not possible	Not possible
1039	1/2	835	−0.03 or −1.7	0 or 2.9
	3/2	835	−0.90 or −2.0	0.80 or 4.0

keV state and the strength of the magnetic field of our electromagnet (≤ 25 kG), we have used a time-integral reversed-field technique (IRF) to measure the g factor of the 204-keV state. Specifically, the method used involves first measuring the unperturbed angular correlation which passes through the level of interest. A transverse magnetic field is then applied, and the coincidence rate for field up and field down is measured at the angle at which the correlation is changing most rapidly. It is most convenient to express the unperturbed correlation as

$$W(\theta) = 1 + B_{22}\cos 2\theta + B_{44}\cos 4\theta .$$

The coincidence rates with the applied field are used to form the ratio

$$R(\theta_0) = \frac{W(\theta_0, B\uparrow) - W(\theta_0, B\downarrow)}{W(\theta_0, B\uparrow) + W(\theta_0, B\downarrow)} ,$$

where B is the applied magnetic field and θ_0 is the fixed angle. For correlations involved in this work where $A_{44} = B_{44} = 0$, θ_0 is 45, 135, 225°, etc., the analytic expression for $R(\theta_0)$ becomes (provided there are no other perturbations present)

$$R(^{135^\circ}_{225^\circ}) = \mp 2B_{22}\omega\tau/[1 + (2\omega\tau)^2], \qquad (1)$$

where $\omega\tau = -g(\mu_N/\hbar)B\tau$ and B_{22} is the angular-correlation coefficient uncorrected for geometry.

Two fixed and one movable 7.6-cm×7.6-cm NaI(Tl) detectors were used in the g-factor measurement. The 204-keV γ ray was detected in the movable counter in order to enable us to make four simultaneous measurements of the g factor (from both the 582-204 and 835-204 cascades in each fixed detector). Unperturbed angular correlations were measured for five angles in the magnet. The rather large detector distance of 14 cm was chosen so as to increase the asymmetry and to reduce the effect of the fringing field when the magnet was turned on. The coincidence rates at the fixed angle were recorded over a period of 10 days, as the applied magnetic field was reversed every hour. Singles rates in the 204-keV counter were found to be constant to within 0.3% for the unperturbed measurements and varied less than that for the measurements with field. The geometrical arrangement of the three detectors was chosen so that for the applied-field measurements the fixed angles were 135 and 225°. This provided a check as to the reliability of the IRF method, since the coincidence rate should increase in one detector and decrease in the other as the field is applied [see Eq. (1)]. For both field and no-field measurements, lead was placed on the face of the high-energy detectors. Small scattering corrections were made, but no correction was made for the 835-keV Compton contribution to the 582-keV γ ray.

Results for the four cascades which were measured are shown in Table VI. The unperturbed correlations in the magnet, if corrected for geometry and Compton contributions, were consistent with the unperturbed correlations which were found outside the magnet. The weighted average for $\omega\tau$ was $\omega\tau = -g(\mu_N/\hbar)B\tau = +0.0280 \pm 0.0017$. A Rawson rotating-coil flux meter was used to measure the applied magnetic field, and the field was found to be 20.6 ± 0.4 kG. Niobium foil is cubic, and hence, paramagnetic corrections were assumed to be negligible; thus the weighted average for the experimentally determined quantity $g\tau\mu_N/\hbar$ was $(-1.360 \pm 0.082)\times 10^{-6}$/G. Dividing by the mean life which we found, $\tau = 1.09 \pm 0.02$ nsec, and evaluating the constants, we find $g = -0.26 \pm 0.02$ for the metallic source. The result for the liquid source was $g = -0.30 \pm 0.04$, but because of the possibility of attenuation in that source we have used only the niobium-foil result. Our result is not in agreement with the previously measured value of Andrade *et al.*,[14] also found by the IRF method, of $g = -0.37 \pm 0.03$.[35] Recently, another measurement of the g factor, using an external field of 50.5 kG has been reported.[13] The result of $g = -0.30 \pm 0.02$ just straddles our value and also disagrees with Andrade *et al.*[14]

Nuclear Structure of Mo^{95}

Before considering models which have attempted to explain the general level structure of Mo^{95}, it is instructive to apply two rather simple models to the ground and first excited states. The core-excitation model of de-Shalit[36] treats the ground state as a single $d_{5/2}$ neutron and the first excited

TABLE VI. Data for g-factor measurement.

	Counter No. 1		Counter No. 2	
	582 – 204	835 – 204	582 – 204	835 – 204
B_{22}	−0.188 ± 0.004	−0.135 ± 0.005	−0.195 ± 0.004	−0.133 ± 0.005
B_{44}	−0.002 ± 0.002	−0.004 ± 0.003	+0.001 ± 0.002	−0.009 ± 0.003
θ_0(deg)	135°	135°	225	225
$R(\theta_0)$	+0.0101 ± 0.0010	+0.0090 ± 0.0013	−0.0112 ± 0.0010	−0.0062 ± 0.0014
$\omega\tau$	+0.0268 ± 0.0027	+0.0333 ± 0.0052	+0.0288 ± 0.0027	+0.0233 ± 0.0052

TABLE VII. Moments and transition rates for Mo^{95}.

	Experimental	Ref.	Core Exc	$3d_{5/2}$	Vervier[a]	CC[b]	KK
$B(E2,\ 3/2\rightarrow 5/2)\ (e^2b^2)$	0.053 ± 0.005	28	0.056	0.016	0.089	0.057	0.015
$B(E2,\ 7/2\rightarrow 5/2)\ (e^2b^2)$	0.005 ± 0.003	29	...	...	...	0.042	0.007
$B(E2,\ 1/2\rightarrow 5/2)\ (e^2b^2)$	0.060 ± 0.015	c	...	...	...	0.045	0.042
$B(M1,\ 3/2\rightarrow 5/2)\mu_N{}^2$	0.0044 ± 0.0006	28	0	0	0.008	0.0016	...
g(ground)	-0.364 ± 0.001	d	$\equiv -0.36$	$\equiv -0.36$	−0.48	−0.38	...
g(204 keV)	-0.28 ± 0.02		−0.26	−0.36	−0.48	−0.38	...
Q(ground) (b^2)	$+0.12\pm0.03$	e	...	...	...	+0.086	...

[a]See Ref. 17.
[b]See Ref. 18.
[c]D. G. Alkhazov, K. I. Erokhina, and I. K. Lemburg, Izv. Akad. Nauk SSSR Ser. Fiz. 28, 1667 (1964) [transl.: Bull. Acad. Sci. USSR, Phys. Ser. 28, 1559 (1964)].
[d]I. Lindgren, in *Alpha-, Beta-, and Gamma-Ray Spectroscopy*, edited by K. Siegbahm (North-Holland Publishing Company, Amsterdam, The Netherlands, 1965), p. 1621.
[e]A. Narath and D. Alderman, Phys. Rev. 143, 328 (1966).

state as this particle coupled to a core excitation. The other model, suggested by Talmi,[37] considers both the $\frac{5}{2}+$ ground state and $\frac{3}{2}+$ excited state to be due to three $d_{5/2}$ neutrons coupled to different spins. In Table VII we show the $B(E2)$ and $B(M1)$ transition rates from the 204-keV level to the ground state and the magnetic moment of the 204-keV level, as predicted by these models. In calculating the magnetic moment, we have taken the experimental value of the ground-state magnetic moment and have chosen $g_c = Z/A$ for the core g factor. It appears that, at least from these quantities, the 204-keV level resembles more the simple particle-plus-core excitation.

Neither of these models can adequately treat many levels of Mo^{95}, so we shall turn to more extensive calculations. Kisslinger and Sorensen (KS),[15] using a pairing-plus-quadrupole interaction, first predicted levels of Mo^{95} in a paper which investigated spherical nuclei over a large region of the Periodic Table. Figure 8(a) shows the experimental energy levels of Mo^{95}, and Fig. 8(b) gives the KS predictions. The energy level density at about 800 keV agrees quite well with experiment; however, the failure to predict a low-lying $\frac{3}{2}+$ state and the appearance of low-lying $\frac{1}{2}+$ state are major failures of the theory. The KS prediction for both the ground-state magnetic dipole moment and electric quadrupole moment are not in agreement with experiment. Their interpretation of the general failure of the calculations for odd-mass nuclei in the region around $A = 95$ was that isotopes in this region had a great instability for the spherical shape, and thus their coupling scheme was breaking down.

Bhatt and Ball[16] and Vervier[17] have used Talmi's

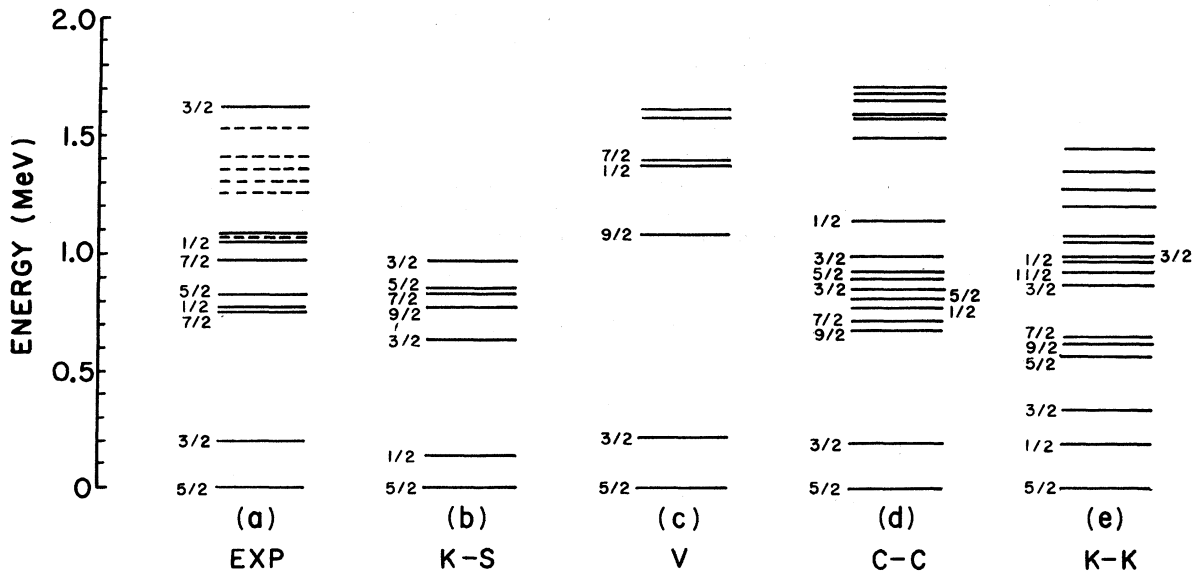

FIG. 8. (a) Represents the levels of Mo^{95} observed in experiments, (b) represents the levels calculated by Kisslinger and Sorensen, (c) by Vervier, (d) by Choudhury and Clemens, and (e) is based on the Kisslinger and Kumar model.

theory of effective interaction to calculate the levels of Mo^{95}. Single-particle levels of $g_{9/2}$ for protons and $d_{5/2}$ for neutrons were used in the calculation. Effective p-p, p-n, and n-n interactions were derived from experimental spectra of $_{42}Mo^{95}_{53}$, $_{41}Nb^{92}_{51}$, and $_{40}Zr^{92}_{52}$, and the interaction of the three $d_{5/2}$ neutrons was obtained from the energy spectrum of $_{40}Zr^{93}_{53}$. While the calculation [see Fig. 8(c)] successfully accounts for the low-lying $\frac{3}{2}+$ state, the next group of levels is much too high in energy. Results of this calculation for certain moments and transition rates are shown in Table VII. Vervier concluded that his calculation could be improved by the inclusion of more single-particle levels, since (d,p) reactions have shown that more than just the $d_{5/2}$ shell is important for Mo^{95}.

The most recently published calculations concerning Mo^{95} are those of Choudhury and Clemens.[18] They employ a coupling scheme in which the quadrupole vibrations of an even-even core are coupled to shell-model particles or holes. The coupling strength, the number of phonons, and the shells that are included in the calculations are varied to obtain the best agreement with experiment for each isotope. In order to obtain the best fit for Mo^{95}, they find they must couple two configurations of three nucleons to the Mo^{98} core, three $d_{5/2}$ neutron holes coupled to spin $\frac{5}{2}$, and three $d_{5/2}$ neutron holes coupled to spin $\frac{3}{2}$. Their results for the energy levels of Mo^{95} are shown in Fig. 8(d). Although there does not appear to be experimental evidence for the doublets at 822 and 1039 keV calculated by Choudhury and Clemens, the over-all fit to the experimental energy levels is the best of any of the previous calculations. Predictions of this model for moments and transition rates are shown in Table VII. In order to fit the previous magnetic-moment result, an effective spin g factor was used. With the exception of $B(E2, \frac{7}{2} \rightarrow \frac{5}{2})$ and the g factor of the 204-keV level, the results are very close to experimental values. However, although the fit to the Mo^{95} data is so good, there are some unsatisfactory points about the model. In light of the stripping data,[9] it is quite surprising that the model does so well, since it considers only one shell-model level. Also, the selection of the number of phonons and the particle configurations which are included in the calculation seems to be rather arbitrary.

Kisslinger and Kumar (KK)[19] found that they could at least partially account for the experimentally observed rather large static quadrupole moment of the first 2^+ state of certain "spherical" nuclei by the introduction of anharmonicity into the Hamiltonian of Kisslinger and Sorensen. They found they could approximate the effect of the anharmonicity by expressing the "true" nuclear states of the even-even nucleus as linear combinations of the phonon states of the idealized spherical system. If the failure of the KS predictions for Mo^{95} could be attributed to the nonspherical nature of that nucleus, it was thought that the KK theory might better account for its structure.

Calculations with the ODDM code were carried out for odd-mass nuclei in the region $37 \leq Z \leq 43$, $51 \leq N \leq 57$ in order to find the best fit to this mass region. The calculations are similar to the KS calculations with the following major differences. In addition to considering all the shell-model levels between major shell closures, the spin-orbit partners in both the lower and upper shell are included and the amount of mixing of the two-phonon states with the zero- and one-phonon states can be varied. The results of these calculations for Mo^{95} are shown in Fig. 8(e). Although the general density of levels is not too bad, the introduction of anharmonicity has not raised the $\frac{1}{2}+$ level or reduced the $\frac{3}{2}+$ level enough to provide a major improvement over the KS theory for this nucleus. Values of $B(E2)$ for the three lowest levels to the ground state are shown in Table VII. These values are not very close to experiment, and when combined with the rather poor energies of the levels it appears that KK theory is not particularly successful for $_{42}Mo^{95}_{53}$ (nor is it successful for $_{40}Zr^{93}_{53}$). There are several possible modifications which might improve the theory in this region. Three quasiparticle intruder states[38] should perhaps be included, the coupling strength of KS may need to be changed, and spin-dependent forces may be necessary.[39] Further discusssion of this theory over a more extended mass region will be found in a future article.[40]

Hyperfine Fields

A liquid source of Tc^{95m} was prepared by the method described above. This source was then deposited upon a 5-mil iron foil and a 30-mil nickel foil and evaporated to dryness. The foils were placed on a tantalum support, heated to 900°C in a hydrogen atmosphere for a period of one week, and were then cleaned with emory paper and soaked in Radiacwash for a period of several hours. Although the results for the hyperfine fields seemed satisfactory with these samples, we would have liked to melt each sample. However, no furnace of sufficient power, where a radioactive sample could be melted, was available.

For the measurement of the hyperfine fields three NaI(Tl) detectors were used. A fixed counter, which detected the 204-keV γ ray, and two movable counters were used to measure the 582-204-keV and 835-204-keV time-integral angular correlations. In addition to measuring the angle

of precession of the angular correlations with a transverse polarizing field applied to the ferromagnetic foils, the angular correlations in an unattenuated niobium foil and in the iron foil with no polarizing field were measured. During measurements with the applied field the foils reached an equilibrium temperature of 55°C.

Although both the 582-204 and 835-204 cascades were measured, the former gave much more consistent results because of its greater anisotropy, its somewhat greater intensity, and the fact that because it consists of a single γ ray; and peak shifts due to the magnetic field are easier to correct for in that cascade. Thus the results below are for the 582-204 cascades uncorrected for the Compton contribution of the 835-keV γ ray but corrected for the small amount of scattering (see above).

Attenuation of the time-integral angular correlation due to a randomly oriented field gives the magnitude but not the sign of $\omega\tau$.[41] For the 5-mil iron foil, the experimental attenuation with no polarizing field of $G_2 = 0.85 \pm 0.06$ results in $|\omega\tau| = 0.30 \pm 0.08$. We have assumed that demagnetizing the foil left it without any net polarization direction.

The time-integral angular correlation results in the iron foil with a transverse polarizing field of 1.3 kG applied are shown in Fig. 9. They were fitted to

$$W(\theta, B) = 1 + \sum_{2,4} \frac{B_{nn}}{1+(n\omega\tau)^2} \cos\left[n\left(\theta - \frac{\tan^{-1} n\omega\tau}{n}\right)\right]$$

by a least-squares method. Values of B_{22} were found to be consistent with the unattenuated niobium-foil measurements. For the 582-204 cascades, the average value of $\omega\tau$ was found to be $\omega\tau = -g(\mu_N/\hbar)B\tau = -0.319 \pm 0.016$. The effective field is found by dividing this result by the quantity

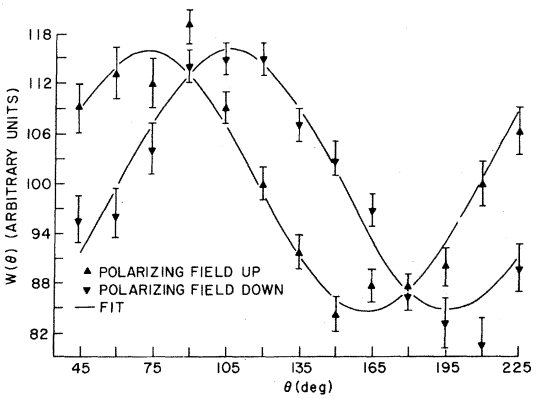

FIG. 9. Perturbed angular correlation of the 582-keV-204-keV cascade with the source of Tc^{95m} diffused into an iron foil.

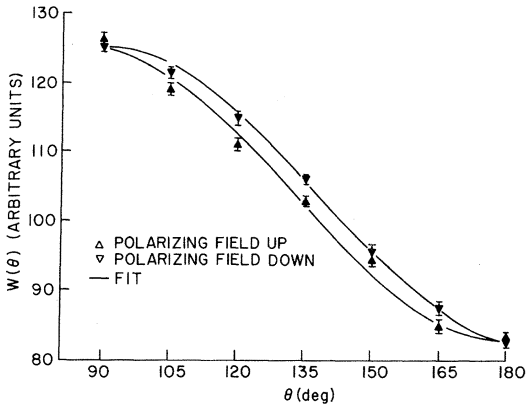

FIG. 10. Perturbed angular correlation of the 582-keV-204-keV cascade with the source of Tc^{95m} diffused into nickel foil.

found in the g-factor measurement of $g\tau(\mu_N/\hbar) = (-1.360 \pm 0.082) \times 10^{-6}$/G and then correcting for the external field. We find B_{eff}(Mo in Fe) = $-236\,000 \pm 19\,000$ G at 55°C, where the negative sign indicates the hyperfine field is opposite to the externally applied field.

In order to roughly compare this result with the spin-echo result at 4.2°K, we correct for the temperature difference by the Bloch $T^{3/2}$ law for iron[42] and find that the perturbed angular-correlation result gives B_{eff}(Mo in Fe) = $-242\,000 \pm 20\,000$ G at 4.2°K. This result is in rather good agreement with the spin-echo result of $-256\,000 \pm 5\,000$ G.[20] The time-integral technique which we have used will in general result in a lower value of the magnetic field because the technique will average over the different orientations of the fields in a nonuniform sample.

One of the perturbed 582-204 correlations in a 30-mil nickel foil with a polarizing field of 1.3 kG is shown in Fig. 10. The average value of $\omega\tau$ for the 582-204 cascades is $\omega\tau = -0.0389 \pm 0.0067$ rad. This results in an effective field of B_{eff}(Mo in Ni) = $-29\,900 \pm 5\,100$ G at 55°C. There is some question as to whether the polarizing field was sufficient to saturate this sample, so that our result should be taken as a lower limit for the field.

Recently another measurement has been made of these internal fields.[13] No data were presented, but we can extrapolate their values for the shifts to be about $\omega\tau = -0.35$ for Mo in Fe and $\omega\tau = -0.54$ for Mo in Ni, somewhat larger than we obtained.

Our results for Mo in Fe and Ni hosts generally confirm the trend in the hyperfine field empirically predicted by Shirley, Rosenblum, and Matthias[20] from the conduction-electron-polarization mechanism suggested by Daniel and Friedel.[43] The agreement with the conduction-electron-polarization prediction indicates the absence of any sizable

local moment in molybdenum.

ACKNOWLEDGMENTS

We wish to thank L. S. Kisslinger for the use of his code ODDM and for many helpful discussions. Appreciation is also expressed to J. D. McGervey for his many helpful discussions, to R. W. Bercaw and T. Fessler for permitting us to use the facilities at the National Aeronautical and Space Administration-Lewis Research Center, to Margery Ratner for programming assistance, and to J. M. Arnold and W. R. Owens for aid in data taking.

---

†From a dissertation submitted by Peter Bond in partial fulfillment of the requirements of the Ph.D. degree at Case Western Reserve University, 1969.

*Now at Department of Physics, Stanford University, Stanford, California.

‡Now at Physics Department, University of Cincinnati, Cincinnati, Ohio.

[1]R. Cesareo, H. Langhoff, and A. Flammersfeld, Z. Physik 197, 426 (1966).

[2]J. P. Unik and J. O. Rasmussen, Phys. Rev. 115, 1687 (1959).

[3]B. S. Dzhelepov, G. S. Katykhin, V. E. Maidanyuk, and A. I. Feoktistov, Izv. Akad. Nauk SSSR Ser. Fiz. 27, 172 (1963) [transl.: Bull. Acad. Sci. USSR Phys. Ser. 27, 184 (1963)].

[4]T. Cretzu, K. Hohmuth, and J. Schintlemeister, Nucl. Phys. 70, 129 (1965).

[5]G. Chilosi, E. Eichler, and N. K. Aras, Nucl. Phys. A123, 327 (1969).

[6]S. A. Hjorth and B. L. Cohen, Phys. Rev. 135, B920 (1964).

[7]H. Ohnuma and J. L. Yntema, Phys. Rev. 178, 1855 (1969).

[8]C. F. Moore, P. Richard, C. E. Watson, D. Robson. and J. D. Fox, Phys. Rev. 141, 1166 (1966).

[9]J. B. Moorehead and R. A. Moyer, Phys. Rev. 184, 1205 (1969).

[10]B. Van Nooijen, H. Van Krugten, and G. B. Vingiani, Physica 28, 644 (1962).

[11]A. Aoki, J. Phys. Soc. Japan 16, 1086 (1961).

[12]P. Da. R. Andrade, A. Maciel, J. D. Rogers, J. Wirth, and F. C. Zawislak, Nucl. Phys. 77, 298 (1966).

[13]W. Meiling and F. Stary, Nucl. Phys. 74, 113 (1965).

[14]E. Gerdau *et al.*, Annual Report, 1966, Institute fur Experimental Physik, Physikalisches Statsinstitut, Hamburg, Germany, 1968 (unpublished).

[15]L. S. Kisslinger and R. Sorensen, Rev. Mod. Phys. 35, 853 (1963).

[16]K. H. Bhatt and J. B. Ball, Nucl. Phys. 63, 286 (1965).

[17]J. Vervier, Nucl. Phys. 75, 17 (1966).

[18]D. C. Choudhury and J. T. Clemens, Nucl. Phys. A125, 140 (1969).

[19]L. Kisslinger and K. Kumar, Phys. Rev. Letters 19, 1239 (1969).

[20]D. A. Shirley, S. S. Rosenblum, and E. Matthias, Phys. Rev. 170, 363 (1968).

[21]25-cc detector supplied by Princeton Gamma Tech and 40-cc detector supplied by Nuclear Diodes.

[22]T. Matsuo, J. M. Matuszek, N. D. Dudley, and T. T. Sugihara, Phys. Rev. 139, B886 (1965).

[23]R. Cesareo, L. Frevert, and A. Flammersfeld, Z. Physik 205, 174 (1967).

[24]N. K. Aras, E. Eichler, and C. G. Chilosi, Nucl. Phys. A112, 609 (1968).

[25]C. M. Lederer, J. M. Hollander, and I. Perlman, *Table of Isotopes* (John Wiley & Sons, Inc., New York, 1967), 6th ed.

[26]C. Williamson and J. P. Boujot, CERN Report No. CEA 2189 (unpublished).

[27]J. Owen and I. M. Ward, Phys. Rev. 102, 591 (1956).

[28]F. K. McGowan and F. H. Stelson, Phys. Rev. 109, 901 (1958).

[29]H. Langhoff, R. Cesareo, and A. Flammersfeld, Z. Physik 205, 1 (1967).

[30]R. E. Bell, in *Alpha-, Beta-, and Gamma-ray Spectroscopy*, edited by K. Siegbahn (North-Holland Publishing Company, Amsterdam, The Netherlands, 1965), p. 905.

[31]Harshaw integral assemblies.

[32]E. B. Shera and K. J. Casper, Nucl. Instr. Methods 17, 174 (1962).

[33]Cosmic Radiation Laboratories, Inc.

[34]M. J. L. Yates, in *Alpha-, Beta-, and Gamma-ray Spectroscopy*, edited by K. Siegbahn (North-Holland Publishing Company, Amsterdam, The Netherlands, 1965), p. 1691.

[35]This value has been recalculated using the more recent value of the mean life.

[36]A. de Shalit, Phys. Rev. 122, 1530 (1961).

[37]I. Talmi, Rev. Mod. Phys. 34, 704 (1962).

[38]L. S. Kisslinger, Nucl. Phys. 78, 341 (1966).

[39]L. S. Kisslinger, Nucl. Phys. 35, 114 (1962).

[40]L. S. Kisslinger, K. Kumar, and P. D. Bond, to be published.

[41]E. Matthias, S. S. Rosenblum, and D. A. Shirley, Phys. Rev. Letters 14, 46 (1965).

[42]C. Kittel, *Introduction to Solid State Physics* (John Wiley & Sons, Inc., New York, 1967), 3rd ed., p. 461.

[43]E. Daniel and J. Friedel, J. Phys. Chem. Solids 24, 1601 (1963).